Journal of Integrative Agriculture 2026, 25(7): 2970–2981

Available online at ScienceDirect

Journal of Integrative Agriculture



RESEARCH ARTICLE

Marek's disease virus inhibits the JAK–STAT signaling pathway to evade the innate immune response

Tong Zhou[1], Peidong Guo[1], Li Gao[1], Rui Liu[1], Changjun Liu[1], Yanping Zhang[1], Hongyu Cui[1], Xiaole Qi[1], Yongzhen Liu[1], Suyan Wang[1], Yuntong Chen[1], Yulu Duan[1], Xiaomei Wang[1, 4], Yulong Gao[1#], Kai Li[1, 2, 3#]

[1] *Avian Immunosuppressive Diseases Division, State Key Laboratory for Animal Disease Control and Prevention, Harbin Veterinary Research Institute, Chinese Academy of Agricultural Sciences, Harbin 150069, China*
[2] *Institute of Urban Agriculture, Chinese Academy of Agricultural Sciences, Chengdu 610213, China*
[3] *Chengdu National Agricultural Science and Technology Center, Chengdu 610213, China*
[4] *Jiangsu Co-innovation Center for Prevention and Control of Important Animal Infectious Disease and Zoonoses, Yangzhou University, Yangzhou 225009, China*

Highlights

- Marek's disease virus (MDV) reduced interferon-stimulated genes (ISGs) production by inhibiting signal transducer and activator of transcription 1 (STAT1) nuclear translocation.
- Meq reduced interferon-stimulated response element (ISRE) promoter activity and inhibited STAT1 phosphorylation.
- Meq interacted with JAK1 and tyrosine kinase 2 (TYK2) and inhibited JAK1–STAT1 interactions.
- Meq degraded TYK2 *via* a caspase-mediated pathway.
- Meq-deficient MDV replicated less efficiently than wild-type MDV.

Abstract

The Janus kinase (JAK)–signal transducer and activator of transcription (STAT) signaling pathway plays a crucial role in innate immunity by inducing antiviral proteins in response to interferon signals. Marek's disease virus (MDV), a member of the alphaherpesvirus family, exerts potent tumorigenic and immunosuppressive effects. Recent studies have primarily focused on the tumorigenic mechanisms of MDV, and the mechanism of immune evasion has not been fully understood. In this study, we showed that MDV reduced the production of interferon-stimulated genes (ISGs) by inhibiting the phosphorylation and nuclear translocation of STAT1. Using a dual-luciferase reporter system, we screened for viral proteins that significantly suppress interferon-stimulated response element (ISRE) promoter activity. Meq overexpression markedly reduced ISRE promoter activity and ISG expression, whereas infection with Meq-deficient MDV induced higher ISG production *in vitro* and *in vivo* than infection with wild-type MDV. Meq also inhibited the phosphorylation and nuclear translocation of STAT1. Further experiments showed that Meq interacted with JAK1 and tyrosine kinase 2 (TYK2) and thereby inhibited JAK1–STAT1 interactions. Meq degraded TYK2 *via* a caspase-mediated pathway. The Meq-deficient MDV mutant replicated less efficiently than the wild-type MDV, both *in vitro* and *in vivo*. Collectively, these findings demonstrate that Meq played an immunosuppressive role in MDV by attenuating the JAK–STAT signaling pathway, which facilitated escape from innate immune surveillance mechanisms.

Keywords: Marek's disease, JAK–STAT, innate immunity, immune evasion, interferon-stimulated gene

1. Introduction

Marek's disease (MD) is a profoundly malignant and fatal disease caused by Marek's disease virus (MDV) that poses a severe threat to the poultry industry. The prevalence of this global malady is escalating, inflicting huge economic losses annually (Morrow and Fehler 2004). MD presents two primary risks to the poultry sector. The direct risk is due to its marked tumorigenicity, resulting in the development of multiple types

Received 26 June 2024; Received in revised form 19 September 2024; Accepted 8 October 2024; Available online 6 November 2024
#Correspondence Yulong Gao, E-mail: gaoyulong@caas.cn; Kai Li, Tel: +86-451-51051694, Fax: +86-451-51997166, E-mail: likai01@caas.cn

© 2026 CAAS. Publishing services by Elsevier B.V. on behalf of KeAi Communications Co. Ltd. This is an open access article under the CC BY-NC-ND license (http://creativecommons.org/licenses/by-nc-nd/4.0/). Peer review under responsibility of Editorial Board of *Journal of Integrative Agriculture*.
doi: 10.1016/j.jia.2024.11.019

of cancer and the eventual death of infected chickens. The indirect risk arises from the virus's immunosuppressive traits, predisposing vaccinated individuals to immune incompetence and susceptibility to secondary bacterial and viral infections (Conradie *et al.* 2019). Despite the historical efficacy of vaccination in managing MD over the past five decades, the ongoing evolution and virulence of MDV strains remain the foremost impediments to sustaining effective disease control (Davidson 2020).

Evading the host's innate immune response is a pivotal strategy employed by herpesviruses to effectively establish infection, latency, and persistence within a host (Beachboard and Horner 2016). Recognition of an invading pathogen by diverse pattern-recognition receptors within the host initiates an innate immune response. These receptors bind to conserved pathogen-associated molecular patterns that trigger the production of type I interferons (IFNs) and other antiviral factors (Wu and Chen 2014; Brubaker *et al.* 2015). The type I IFN response, orchestrated by an array of interferon-stimulated genes (ISGs), is the principal defense mechanism against viral incursion, replication, and dissemination. Type I IFNs elicit ISG expression by activating the Janus kinase (JAK)–signal transducer and activator of transcription (STAT) signaling pathway (Darnell *et al.* 1994; Platanias 2005). Initially, extracellularly secreted type I IFNs bind to IFN receptors (IFNAR1 and IFNAR2) on the cell surface and phosphorylate JAK1 and tyrosine kinase 2 (TYK2), which leads to their activation. Activated JAK phosphorylates the transcription factors STAT1 and STAT2, which assemble into a transcription complex that translocates to the nucleus and instigates the expression of antiviral ISGs (Wang *et al.* 2017). A growing body of evidence indicates that viral infections can subvert IFN responses by either inhibiting IFN induction or impeding the stimulation necessary to induce ISGs (Katze *et al.* 2002; Weber *et al.* 2004; Johnson and Gale 2006; Reid *et al.* 2006).

The viral oncogene Meq, which encodes a leucine zipper DNA-binding protein, has been extensively investigated in MDV-induced tumorigenesis (Davidson 2020). Meq comprises a basic leucine zipper (bZIP) domain at the N terminus and a proline-rich transactivation domain at the C terminus (Qian *et al.* 1995; Liu *et al.* 1999; Ross 1999). Substantial research has been devoted to elucidating the transcriptional activity of Meq (Qian *et al.* 1996; Liu and Kung 2000). Meq influences the expression of both cellular and viral genes by dimerizing with cellular transactivators such as cellular Jun (c-Jun), cellular Myc (c-Myc), and C-terminal binding protein (CtBP), all of which also harbor a bZIP domain. Previous findings have shown that a chicken fibroblast cell line (DF-1) can be used to validate the transformative potential of Meq (Levy *et al.* 2005). Meq upregulates transformation-related genes belonging to the v-Jun transforming pathway, indicating that the transformative capacity of Meq operates through the Jun pathway. Furthermore, Meq can downregulate the anti-apoptotic genes Fas antigen and Death-associated protein 5, suggesting their involvement in promoting the apoptosis of immune cells (Jarosinski *et al.* 2006). Additionally, Meq can impede the recruitment of TANK-binding kinase 1 and IFN regulatory factor 7 (IRF7) to the STING complex, thereby inhibiting IRF7 activation and IFN-β induction (Li *et al.* 2019).

The objective of this study was to identify MDV proteins that suppress the JAK–STAT pathway and unravel their associations with viral replication. Our findings indicate that the MDV oncogene Meq plays a pivotal role as a suppressor of the JAK–STAT pathway. At the mechanistic level, Meq binds to JAK1 and TYK2, resulting in impaired STAT1 phosphorylation, dimerization, and nuclear localization. This impairment impeded the effective induction of antiviral genes following MDV infection. Our findings reveal a novel strategy employed by MDV to evade host innate immunity and shed light on the mechanisms underlying the establishment of its incubation period and transformation.

2. Materials and methods

2.1. Animals

In this study, we used specific pathogen-free (SPF) chickens and fertilized SPF chicken eggs, which were purchased from the State Resource Center of the Laboratory Animal for Poultry (Harbin, China). Ten-day-old SPF chicken embryos were used to prepare primary chicken embryonic fibroblasts (CEFs).

2.2. Cells, viruses, and antibodies

DF-1 cells (ATCC CRL-12203) were cultured in Dulbecco's modified Eagle's medium (DMEM; Life Technologies, Grand Island, NY, USA) containing 10% fetal bovine serum (FBS; Sigma-Aldrich, St. Louis, MO, USA). Primary CEFs were prepared from 10-day-old SPF chicken embryos. CEFs were cultured in DMEM supplemented with 10% FBS (Sigma-Aldrich). The virulent MDV-Georgia strain (GA) (GenBank accession number AF147806) and HVT FC126 strain (GenBank accession number AF291866) were propagated in CEFs before use. The rGA-dMeq strain was provided by our laboratory. Antibodies, including mouse anti-Flag, mouse anti-hemagglutinin (HA), rabbit anti-HA, mouse anti-c-Myc, rabbit anti-histone H3, mouse anti-actin (Sigma-Aldrich), rabbit anti-STAT1 (Cell Signaling Technology, Boston, MA, USA), rabbit anti-phospho-STAT1, and rabbit anti-Mx1 (Abcam, Boston, MA, USA) were used, along with mouse anti-gI antibodies, which were prepared in our laboratory. Recombinant chicken (gallus) IFN-β protein was acquired from Cloud-Clone Corp. (USA).

2.3. Plasmid constructs

The MDV open-reading frames (ORFs) were amplified from the genome of the virulent MDV-GA and cloned into the pCAGGS vector with a Flag or HA tag fused to the 3′ end. Plasmids encoding chicken *IFNAR1* (GenBank accession number NM_204859), *IFNAR2* (GenBank accession number NM_001397696), *JAK1* (GenBank accession number NM_204870), *TYK2* (GenBank accession number XM_025145739), *STAT1* (GenBank accession number NM_001012914), and *STAT2* (GenBank accession number XM_040654879) were constructed by cloning the corresponding synthesized sequences into pCAGGS with a c-Myc or HA tag fused to the 3′ end. A chicken ISG promoter luciferase reporter vector (pchISRE-Luc) was constructed by

inserting a fragment of the chicken ISGs promoter into the pGL3-basic vector, as described previously.

2.4. Real-time qPCR analysis

Total RNA was extracted from cells using the RNAiso Plus reagent (TaKaRa, Otsu, Japan). Reverse transcription was performed using HiScript II Q RT SuperMix for qPCR (Vazyme, Nanjing, China). Complementary DNA levels were determined *via* real-time qPCR using Thunderbird SYBR qPCR mix (Lucigen, Madison, WI, USA) and analyzed using a LightCycler 480 system (Roche, Basel, Switzerland). Specific primers for the chicken protein kinase R (*PKR*), myxovirus resistance protein 1 (*Mx1*), zinc finger antiviral protein (*ZAP*), interferon-induced transmembrane protein 3 (*IFITM3*) genes were synthesized by Invitrogen (Shanghai, China), and their relative mRNA expression levels were normalized to that of chicken β-actin mRNA in each sample. The fold differences between the treated and mock samples were calculated. To determine MDV viral titers, total DNA was extracted using the AxyPrep Body Fluid Viral DNA/RNA Miniprep Kit (Corning Life Sciences, Shanghai, China). The total DNA was tested *via* real-time qPCR by measuring the copy numbers of the MDV Meq gene, where the sequences amplified by the Meq primers were present in the MDV-dMeq genome. Expression of the chicken ovotransferrin gene was detected as a reference, as described previously (Sun *et al.* 2017). All control and treated samples were examined in triplicate using samples in the same qPCR plate.

2.5. Transfection and dual-luciferase reporter assays

To determine chicken ISG promoter-binding activity, DF-1 cells seeded in 24-well plates were cotransfected with the interferon-stimulated response element (ISRE)-Luc reporter plasmid and a Renilla luciferase reporter plasmid (pRL-TK), which served as an internal control. The cells were transfected with or without expression plasmids, as indicated, using the TransIT-X2 dynamic delivery system (Mirus, Madison, WI, USA). After transfection for 24 h, the cells were subjected to a 12 h treatment with IFN-β followed by lysis, and then the samples were assayed for firefly and Renilla luciferase activity using the dual-luciferase reporter assay system (Promega, Madison, WI, USA). Relative luciferase activities were normalized to Renilla luciferase activities. The reporter assays were repeated at least three times.

2.6. Coimmunoprecipitation assays and Western blot analysis

Expression plasmids harboring Flag, c-Myc, or HA tags were transfected into DF-1 cells using the TransIT-X2 dynamic delivery system (Mirus). At 48 h post-transfection, cells were lysed in ice-cold Pierce IP buffer (Thermo Fisher Scientific, Waltham, MA, USA) containing a protease inhibitor cocktail (Roche). The lysates were obtained *via* centrifugation and incubated with the indicated antibodies at 4°C for 5 h. Protein G Sepharose beads (Roche) were added, and the samples were incubated for another 6 h. The beads were washed six times with phosphate-buffered saline (PBS) and boiled in sodium dodecyl sulfate-loading buffer before performing Western blot analysis with the indicated antibodies.

For Western blotting, whole-cell lysates were obtained by lysing cells in NP-40 lysis buffer (Beyotime, Beijing, China). Cytoplasmic and nuclear proteins were extracted using the NE-PER nuclear and cytoplasmic extraction reagent (Thermo Fisher Scientific). The protein concentrations were determined using a Bicinchoninic Acid Protein Assay Kit (Thermo Fisher Scientific). Proteins were separated by 12% sodium dodecyl sulfate-polyacrylamide gel electrophoresis, transferred onto nitrocellulose membranes, and incubated with the indicated primary and secondary antibodies. Images were acquired using an Odyssey infrared imaging system (LI-COR Biosciences, Lincoln, NE, USA).

2.7. Confocal microscopy imaging

CEFs were infected with the MDV-GA strain or mock infected for 48 h and then treated with IFN-β for another 12 h. For confocal microscopy imaging, the cells were fixed with 4% paraformaldehyde for 30 min, permeabilized with PBS containing 0.1% Triton X-100 for 15 min, and then blocked with PBS containing 5% bovine serum albumin for 1 h. Next, the cells were incubated with rabbit anti-STAT1 and mouse anti-gI antibodies for 2 h. The cells were washed five times with PBS and incubated with Alexa Fluor 546-anti-mouse and Alexa Fluor 488-anti-rabbit secondary antibodies (Invitrogen). Finally, the nuclei were stained with 4′,6-diamidino-2-phenylindole (DAPI; Sigma-Aldrich). After five washes with PBS, the cells were examined under a confocal microscope (Zeiss LSM880, Oberkochen, Germany).

2.8. Animal experiments

To investigate the effect of MDV-dMeq on replication *in vivo* and the effect of MDV on ISG gene expression *in vivo*, we randomly divided 90 1-d-old SPF chickens into three groups (n=30 per group). Two groups were subcutaneously inoculated with 2000 plaque-forming units (PFUs) of MDV-WT or MDV-dMeq, and the third group was mock-injected with DMEM. On days 3, 7, 10, 14, 21, and 28, five birds from each group were euthanized *via* electronarcosis and cervical dislocation. Spleen samples were collected to analyze chicken ISG expression and viral DNA copy numbers.

2.9. Statistical analysis

All experiments were performed at least thrice unless otherwise indicated; data are presented as the mean±standard deviation. Statistical significance between groups was determined by performing Student's t-test with GraphPad Prism 7.0 software (La Jolla, CA, USA). We set P<0.05 as the threshold for statistical significance.

3. Results

3.1. MDV infection inhibits the JAK–STAT signaling pathway

Initially, we evaluated the antiviral impact of IFN-β on MDV replication *in vitro*. We inoculated the virulent MDV-GA and HVT strains separately into CEFs. We also administered IFN-β at 48 h before or after infection. We measured the MDV copy numbers *via* real-time quantitative polymerase chain reaction

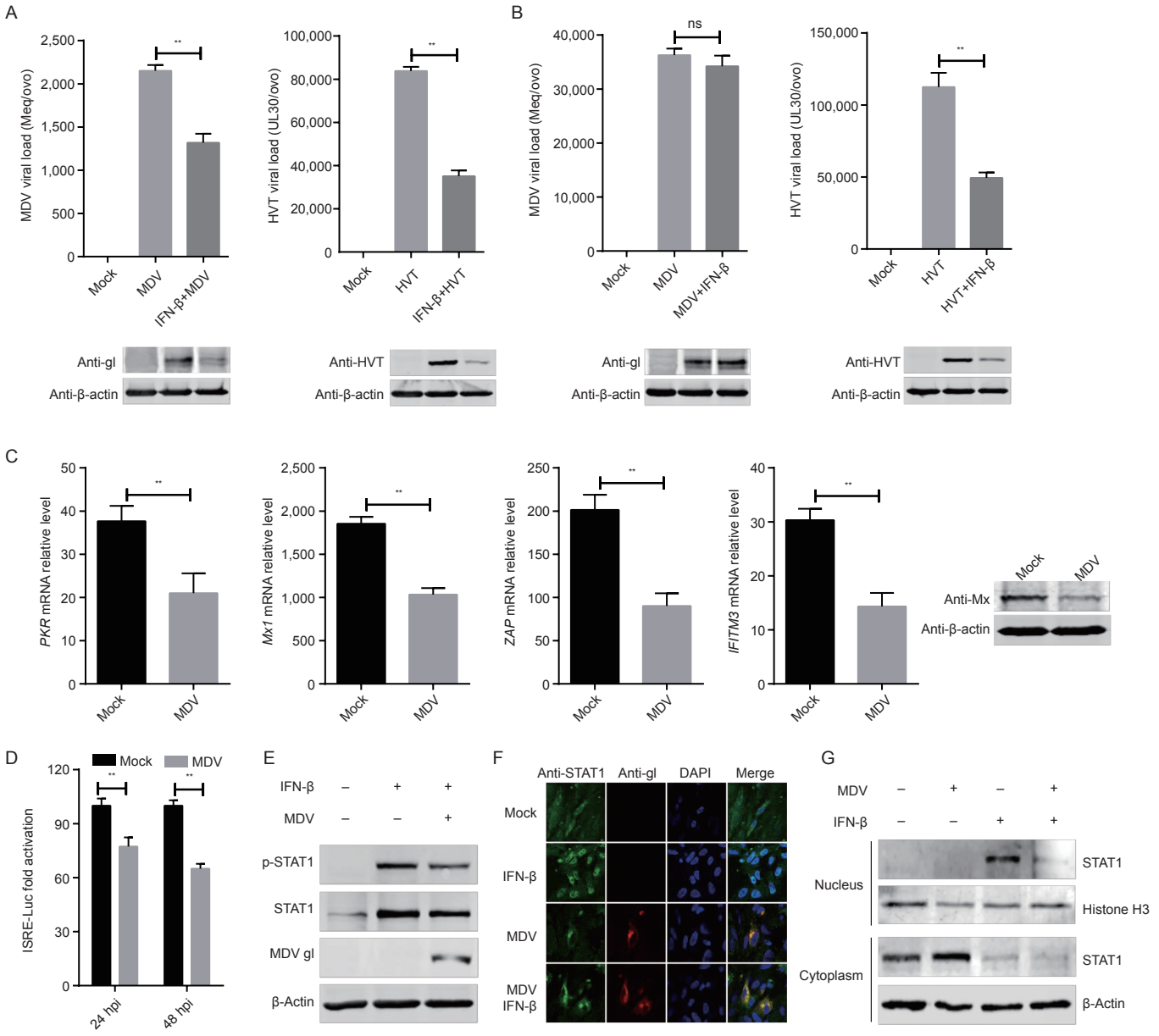


Fig. 1 Marek's disease virus (MDV) infection inhibits the Janus kinase (JAK)–signal transducer and activator of transcription (STAT) signaling pathway. A and B, the embryonic fibroblasts (CEFs) were infected with 100 or 2,000 plaque-forming units (PFUs) of the MDV-Georgia srtain (GA) or HVT FC126 strain or mock infected (using medium alone). The CEFs were treated with IFN-β for 12 h before (A) or after (B) infection. MDV and HVT copy numbers were quantified *via* qPCR at 48 h post-infection (hpi), and the expression levels of the target proteins were detected by Western blotting at 96 hpi. C, CEFs were infected with 100 PFUs of the MDV-GA strain or mock infected and then treated with IFN-β for 12 h. The transcription levels of ISGs were quantified *via* qPCR, and the protein-expression levels of interferon-stimulated genes (ISGs) were detected by Western blotting. *PKR*, protein kinase R; *ZAP*, zinc finger antiviral protein; *Mx1*, myxovirus resistance protein 1; *IFITM3*, interferon-induced transmembrane protein 3. D, CEFs were transfected for 12 h with the ISRE-Luc or TK vector, after which they were inoculated with MDV-GA or empty medium (mock). The inoculated cells were stimulated with IFN-β at 24 and 48 h after inoculation. Samples were collected 6 h after stimulation, and the ISRE-Luc activities were determined with dual-luciferase reporter assays. E, CEFs were either infected with 2,000 PFUs of MDV-GA or mock infected. After 48 h, the cells were stimulated for 1 h with IFN-β and protein samples were collected. The phosphorylation status of STAT1 was detected *via* Western blot analysis. F, CEFs were infected with 500 PFUs of MDV-GA or mock infected for 48 h, after which they were treated with IFN-β for 1 h. The cells were fixed and permeabilized for immunofluorescence analysis. Fluorescence microscopy revealed that MDV-GA (red) influenced the nuclear translocation of STAT1 (green). DAPI staining (blue) was used to visualize the nuclei. Representative images from each experimental group were pooled based on nuclei observed in the same field of view. G, CEFs were infected with 2,000 PFUs of MDV-GA or mock infected for 48 h, followed by treatment with IFN-β for 1 h. Cells were collected for nucleoplasm-separation experiments to assess STAT1 expression. Staining was performed using a STAT1 antibody and a reference antibody. **, $P<0.01$; ns, no significant difference.

(qPCR) analysis. As illustrated in Fig. 1-A, treating CEFs with IFN-β for 12 h before infection led to lower virus titers at 48 h post-infection (hpi) than those found with untreated cells. However, the inhibitory influence of IFN-β on MDV virus titers was entirely nullified if the cells were treated with IFN-β after 48 h of MDV infection (Fig. 1-B). These findings hinted at the

possibility that viral proteins generated during MDV infection may counteract the antiviral properties of IFN-β.

To further explore this phenomenon, we examined the effects of MDV infection on ISG expression. At 48 hpi, the transcription levels of ISGs such as *ZAP*, *IFITM3*, *Mx1*, and *PKR* were significantly lower in CEFs infected with the MDV-GA strain than those in uninfected cells (Fig. 1-C). Additionally, cell lysates from infected and uninfected cells were analyzed with Western blotting. Notably, our findings revealed that Mx1 expression decreased significantly following MDV infection (Fig. 1-C). Furthermore, MDV infection inhibited the activity of the JAK–STAT signaling pathway, resulting in substantial decreases in ISRE promoter activity at both 24 and 48 hpi, when compared with that in uninfected cells (Fig. 1-D). Collectively, these results indicate that MDV replication effectively suppressed IFN-β-induced ISG expression.

To determine how MDV infection suppresses IFN-β signaling, we examined STAT1 phosphorylation following IFN-β stimulation. After IFN-β stimulation, both STAT1 and phosphorylated STAT1 (p-STAT1) were significantly upregulated for a brief duration, when compared with the corresponding levels in the unstimulated group. MDV infection did not impact STAT1 induction, although it did inhibit p-STAT1 induction (Fig. 1-E), indicating that MDV infection hindered STAT1 phosphorylation. Following phosphorylation, STAT1-STAT2 heterodimers form and are translocated to the nucleus to induce ISGs. Minimal STAT1 expression was detected in MDV-infected cells, whereas in uninfected cells stimulated with IFN-β, significant STAT1 induction and subsequent nuclear translocation were observed (Fig. 1-F). However, even after IFN-β stimulation, STAT1 predominantly remained in the cytoplasm in MDV-infected cells (Fig. 1-F), clearly indicating that MDV infection impeded its translocation into the nucleus. The same observation was made during nucleoplasm-separation experiments (Fig. 1-G).

3.2. Multiple MDV proteins inhibit the JAK–STAT signaling

The observed inhibition of ISG production during MDV infection suggests that MDV may encode proteins that antagonize the JAK–STAT signaling pathway. An expression library consisting of 105 MDV genes was used to identify specific MDV proteins responsible for this suppression. Each construct was individually transfected into DF1 cells along with a firefly luciferase reporter plasmid (ISRE-Luc) and a TK reporter plasmid. Subsequently, the cells were treated with IFN-β to assess their responses. Using this assay, we screened for viral proteins capable of inhibiting ISG promoter activation. This screening process successfully identified several MDV proteins, including US3, Meq, and UL42, that reduced IFN-β induction by over 70% (Fig. 2-A). Furthermore, each viral inhibitor suppressed ISG promoter activation in a dose-dependent manner (Fig. 2-B). To validate the inhibitory effects exerted by these selected viral proteins on ISG production, we measured both transcriptional and translational levels of ISGs. Notably, in cells treated with IFN-β, ISG production was significantly lower in the presence of each selected viral protein than that in the absence (Fig. 2-C). Western blot analysis of lysates from cells expressing these viral proteins with subsequent IFN-β stimulation revealed that IFN-β-dependent Mx induction was suppressed when the viral proteins US3, Meq, or UL42 were present (Fig. 2-D). Collectively, these findings strongly indicate that the identified proteins were functionally significant inhibitors of JAK–STAT signal transduction.

3.3. Meq inhibits STAT1 phosphorylation and nuclear translocation

We focused on the MDV protein Meq because it is unique to MDV and is considered a major viral oncoprotein. To confirm the inhibitory effect of Meq on the JAK–STAT signaling pathway, we infected CEFs with wild-type MDV (MDV-WT) or Meq-deficient MDV (MDV-dMeq) for 48 h and stimulated the cells with IFN-β. The ISRE promoter activity and transcription levels of four different ISGs were significantly higher in cells infected with MDV-dMeq than those in cells infected with MDV-WT (Fig. 3-A and B).

Next, we assessed the direct effects of Meq on JAK–STAT signal transduction. First, we examined the effects of Meq on STAT1 phosphorylation. Meq expression in IFN-β-treated CEFs did not alter STAT1 expression, although it significantly impeded IFN-β-induced p-STAT1 levels (Fig. 3-C). STAT1 and STAT2 dimerization was notably inhibited in cells transfected with a Meq-expression plasmid (Fig. 3-D), which followed their phosphorylation. Finally, we investigated whether Meq affected STAT1 nuclear translocation. Untreated DF1 cells predominantly expressed STAT1 in the cytoplasm; however, after IFN-β treatment, STAT1 migration into the nucleus occurred (Fig. 3-E). Notably, IFN-β-treated DF1 cells transiently expressing Meq showed significantly lower STAT1 nuclear translocation than the control transfectants (Fig. 3-E). The same observation was made during nucleoplasm-separation experiments (Fig. 3-F). Furthermore, IFN-β-treated CEFs showed substantially higher nuclear p-STAT1 levels after MDV-dMeq infection than after MDV-WT infection (Fig. 3-G). Collectively, these findings demonstrate that Meq inhibited STAT1 phosphorylation as well as its subsequent dimerization and nuclear translocation.

3.4. Meq interacts with JAK1 and TYK2

The above data suggest that Meq hindered cellular IFN functions by obstructing signaling events downstream of the type-I IFN receptor. To further elucidate the biochemical network of Meq activities, we transiently co-expressed Meq with individual signaling proteins downstream of the type-I IFN receptor and investigated their interactions *via* immunoprecipitation. The results demonstrated that Meq interacts with both JAK1 and TYK2, but not with other host proteins in the JAK–STAT pathway (Fig. 4-A and B). Confocal microscopy analyses revealed that when both Meq and JAK1 or TYK2 were expressed simultaneously in cells, they co-localized in the cytoplasm (Fig. 4-C). These findings indicate that the ability of Meq to downregulate IFN-induced signaling responses may be attributed to its interaction with JAK1 and TYK2. Furthermore, we mapped the interaction

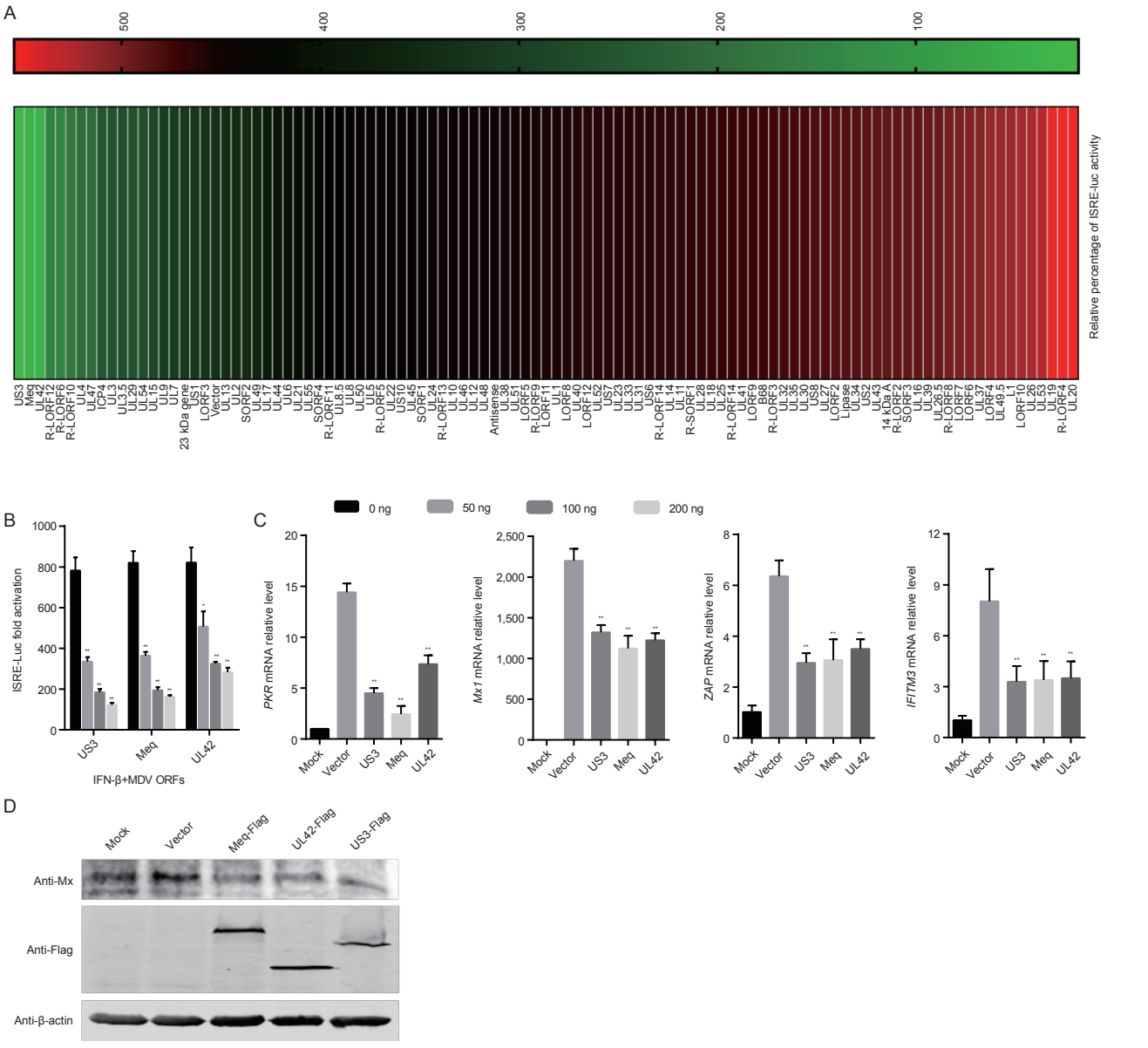


Fig. 2 Screening for Marek's disease virus (MDV) proteins that inhibit the Janus kinase (JAK)–signal transducer and activator of transcription (STAT) signaling pathway. A, heatmap illustrating the impact of MDV open-reading frames (ORFs) on the JAK–STAT pathway. DF1 cells were co-transfected with equal amounts of an interferon-stimulated response element (ISRE) promoter luciferase reporter construct and an MDV ORF expression plasmid or empty vector, followed by stimulation with IFN-β at 48 h post-transfection. Luciferase activities were measured after 6 h of IFN-β stimulation. Higher ISRE promoter activities are represented in red, and lower levels are depicted in green. B, ISRE promoter luciferase activities were assessed by co-transfecting DF1 cells with the ISRE promoter luciferase reporter construct and varying quantities of plasmids encoding the top three MDV ORF inhibitors, followed by IFN-β treatment for 6 h at 48 h post-transfection. C and D, DF1 cells were transfected for 48 h with either the empty vector (pCAGGS) or plasmids encoding the top three MDV ORF inhibitors, after which they were stimulated with IFN-β for 12 h. The interferon-stimulated gene (ISG) mRNA levels were detected with qPCR, and myxovirus resistance protein 1 (*Mx1*) expression was detected by Western blotting. *PKR*, protein kinase R; *ZAP*, zinc finger antiviral protein; *IFITM3*, interferon-induced transmembrane protein 3. *, $P< 0.05$; **, $P<0.01$.

domains of Meq by performing immunoprecipitation experiments and Western blot analysis. We discovered that the C-terminal transactivation domain of Meq (amino acids 122–339) interacted with JAK1, whereas both the N-terminal bZIP domain (amino acids 1–121) and C-terminal domain interacted with TYK2 (Fig. 4-D and E). Collectively, these results support the conclusion that Meq inhibited the JAK–STAT signaling pathway by targeting JAK1 and TYK2.

3.5. Meq blocks the JAK1–STAT1 interaction and degrades TYK2

Recruitment of JAK1 and TYK2 by the type-I IFN receptors, IFNAR1 and IFNAR2, is required for STAT1, STAT2, JAK1, and TYK2 phosphorylation. Our data demonstrated that Meq interacted with JAK1 and TYK2, prompting us to investigate whether Meq could inhibit STAT1 phosphorylation by influencing JAK1–TYK2 interactions, as well as upstream

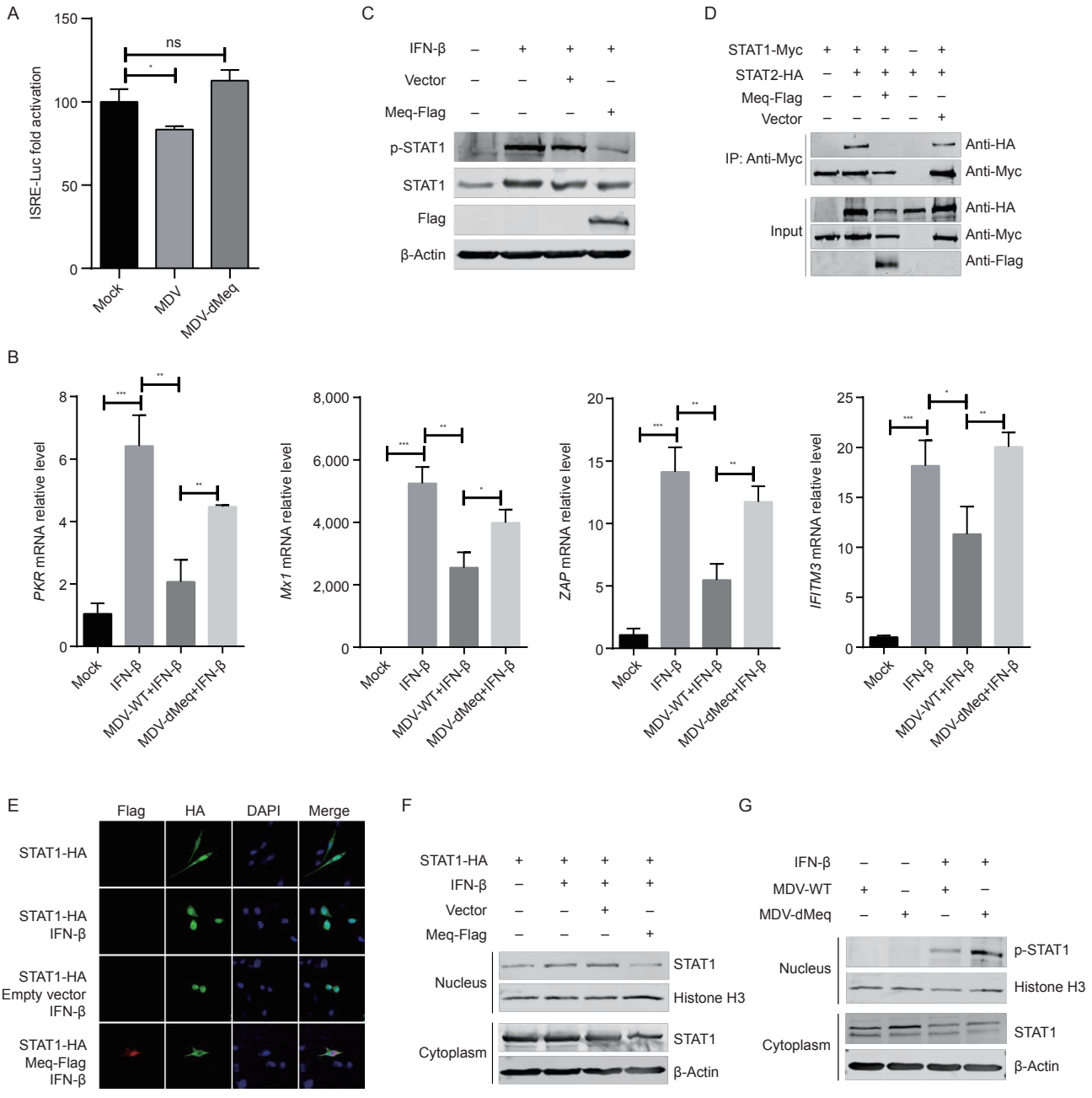


Fig. 3 Effects of Meq on Janus kinase (JAK)–signal transducer and activator of transcription (STAT) signaling activation. A and B, embryonic fibroblasts (CEFs) were treated with empty medium (mock) or 100 PFUs of Marek's disease virus (MDV)-Georgia srtain (GA) or MDV-dMeq for 48 h, after which they were treated with IFN-β. Luciferase activities were assessed after 6 h of IFN-β treatment (A). The transcription levels of interferon-stimulated genes (ISGs) were measured after 12 h of IFN-β treatment (B). PKR, protein kinase R; *ZAP*, zinc finger antiviral protein; *Mx1*, myxovirus resistance protein 1; *IFITM3*, interferon-induced transmembrane protein 3. C, Meq affected STAT1 phosphorylation. DF1 cells were transfected for 48 h with an empty vector or an Meq-Flag vector and then treated with or without IFN-β for 1 h. STAT1 phosphorylation was detected *via* Western blotting. D, Meq affected STAT1-STAT2 dimerization. DF1 cells were co-transfected with plasmids encoding STAT1-Myc, STAT2-HA, or Meq-Flag or an empty vector for 48 h, and then treated with or without IFN-β for 1 h. Immunoprecipitation and Western blot analysis were performed using the indicated antibodies. E and F, Meq affected STAT1 nuclear translocation. DF1 cells were transfected with STAT1-HA, Meq-Flag, or empty vector for 48 h, and treated with or without IFN-β for 1 h. The cells were fixed and permeabilized for immunofluorescence analysis (E). Nucleocytoplasmic separation experiments were conducted to detect the protein expression levels of nuclear and cytoplasmic p-STAT1 along with total STAT (F). G, CEFs were infected with 2,000 PFUs of either MDV-GA or MDV-dMeq for 48 h. After treating the infected cells with IFN-β for 1 h, they were collected to assess the protein expression levels of cytoplasmic and nuclear p-STAT as well as total STAT. *, $P<0.05$; **, $P<0.01$; ***, $P<0.001$; ns, no significant difference.

or downstream elements. To explore this, we treated DF1 cells with IFN-β and co-transfected them with plasmids encoding Meq and either JAK1 and IFNAR2, JAK1 and STAT1, TYK2 and IFNAR1, or TYK2 and STAT2, followed by immunoprecipitation analysis. As depicted in Fig. 5-A, Meq significantly attenuated JAK1–STAT1 interactions, based

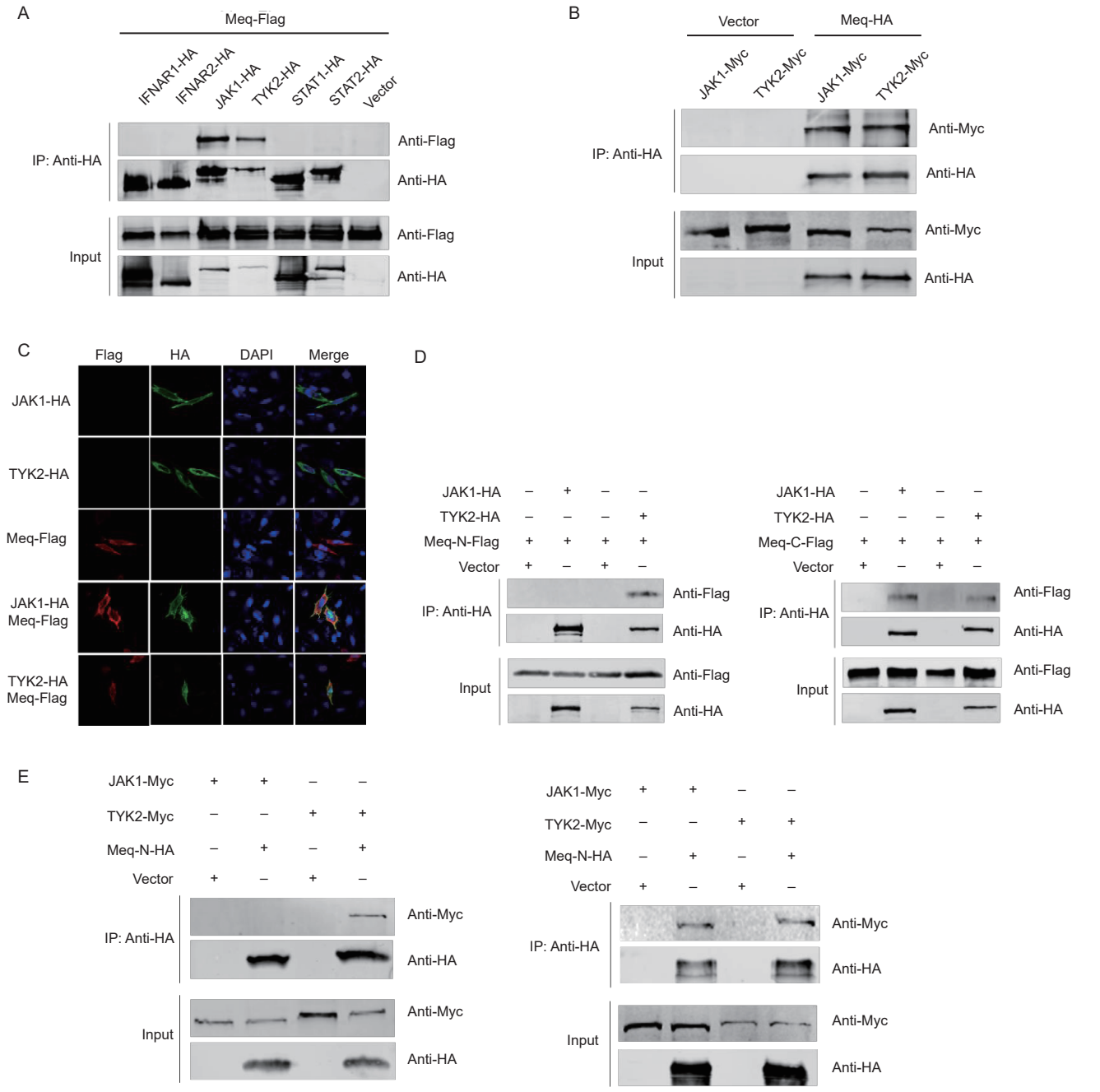


Fig. 4 Meq interacts with Janus kinase 1 (JAK1) and tyrosine kinase 2 (TYK2). A and B, DF1 cells were co-transfected with a Meq-expression vector and the indicated plasmids. After 48 h, the cells were harvested for immunoprecipitation and Western blot analysis using the indicated antibodies. C, DF1 cells were transfected with JAK1, TYK2, and Meq plasmids, either individually or in combination. After 48 h, the cells were fixed and permeabilized for immunofluorescence staining. The colocalization of JAK1, TYK2 (green) and Meq (red) within the cells was observed under a microscope. The nuclei were counterstained with DAPI (blue). D and E, DF1 cells were transfected with a truncated plasmid encoding a truncated Meq variant along with JAK1 and TYK2 plasmids, either alone or in combination. After 48 h, the cells were collected for immunoprecipitation and Western blot analysis using the indicated antibodies.

on a comparison with the control-vector group, whereas the interactions of JAK1 and TYK2 with the other indicated proteins were not affected (data not shown). These findings suggested that Meq inhibited STAT1 phosphorylation by modulating the interaction between JAK1 and STAT1, thereby impeding ISG production.

During the investigation of protein–protein interactions *via* immunoprecipitation analysis, we observed that TYK2 levels were significantly lower in cells overexpressing Meq than in the vector-control group, when using equal plasmid concentrations (Fig. 5-B). We hypothesized that this decrease could reflect altered transcription or translation or accelerated protein-degradation processes that affect TYK2 expression. We performed reverse transcription-qPCR (RT-qPCR) to study changes in TYK2 mRNA level in cells expressing the Meq protein. The endogenous mRNA-expression levels of TYK2

were similar between cells with or without Meq expression (Fig. 5-C), indicating that the TYK2 downmodulation was not due to changes at the transcription level.

Subsequently, we investigated whether the reduced TYK2 expression could be attributed to protein degradation. Typically, cellular proteins undergo degradation through ubiquitin-proteasome-dependent degradation, the autophagy-lysosomal pathway, or caspase-mediated proteolysis. To determine which pathway was involved in Meq-induced TYK2 degradation, we pre-treated DF1 cells with the proteasome inhibitor MG132, the autophagy inhibitors NH_4Cl and 3-methyladenine (3-MA), or the broad-spectrum caspase inhibitor quinoline-Val-Asp-difluoromethyl ketone (Q-VD-OPH) for 12 h and then co-expressed Meq and TYK2 for 24 h. Cell lysates were collected to measure the levels of TYK2. As illustrated in Fig. 5-D, Q-VD-OPH pretreatment significantly inhibited Meq-induced TYK2 degradation, whereas MG132, NH_4Cl, and 3-MA pretreatment did not affect

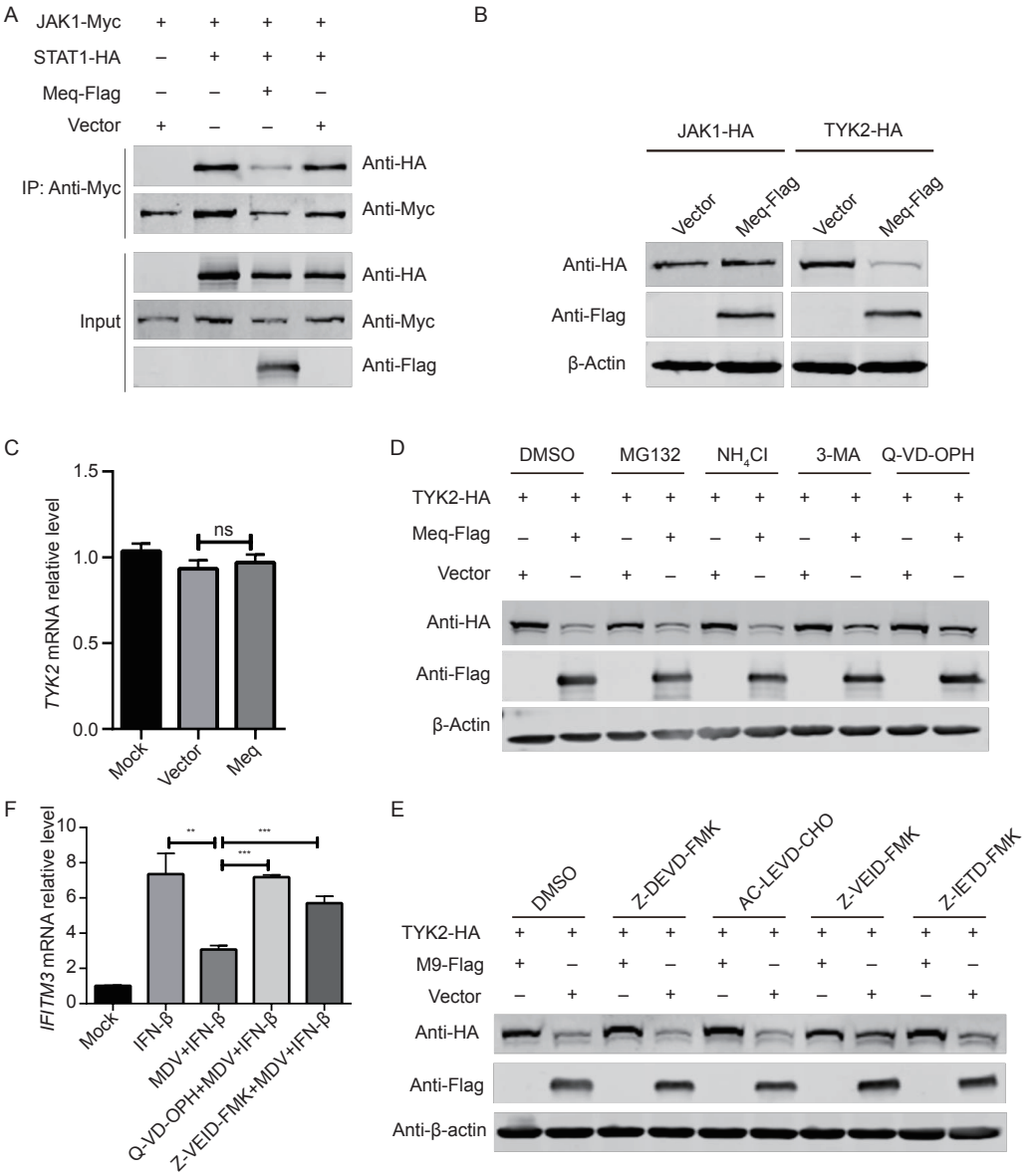


Fig.5 Meq blocks the Janus kinase 1 (JAK1)–signal transducer and activator of transcription 1 (STAT1) interaction and degrades tyrosine kinase 2 (TYK2). A, DF1 cells were transfected for 48 h with the indicated plasmids and then treated for 1 h with IFN-β. Subsequently, the cells were collected for immunoprecipitation and Western blotting using the indicated antibodies. B, DF1 cells were transfected for 48 h with plasmids encoding JAK1 and TYK2, along with the empty vector or Meq plasmid, after which they were harvested for Western blotting. C, DF1 cells were transfected for 48 h with TYK2 along with the empty vector or Meq plasmid, after which *TYK2* mRNA expression was quantitated. D, DF1 cells were transfected with a TYK2 vector and either an empty vector or Meq plasmid; treated for 24 h with dimethyl sulfoxide (DMSO), MG132 (10 μmol L^{-1}), NH_4Cl (20 mmol L^{-1}), 3-methyladenine (3-MA) (10 mmol L^{-1}), or quinoline-Val-Asp-difluoromethyl ketone (Q-VD-OPH) (20 nmol L^{-1}); and harvested for Western blotting. E, DF1 cells were transfected with TYK2 and either an empty vector or Meq plasmid; treated for 24 h with DMSO, Z-DEVD-FMK (100 μmol L^{-1}), AC-LEVD-CHO (30 μmol L^{-1}), Z-VEID-FMK (50 μmol L^{-1}), or Z-IETD-FMK (30 μmol L^{-1}); and harvested for Western blotting. F, CEFs were treated with Q-VD-OPH (20 nmol L^{-1}) or Z-DEVD-FMK (100 μmol L^{-1}) and inoculated with MDV. At 24 h post-infection (hpi), cells were treated with IFN-β for 12 h before the interferon-induced transmembrane protein 3 (*IFITM3*) mRNA level was detected by qPCR. **, $P<0.01$; ***, $P<0.001$; ns, no significant difference.

TYK2 expression. These results indicate that the observed decrease in TYK2 levels was due to caspase-dependent proteolysis.

To further investigate the caspases involved, we added inhibitors of caspase-3 (Z-DEVD-FMK), caspase-4 (AC-LEVD-CHO), caspase-6 (Z-VEID-FMK), and caspase-8 (Z-IETD-FMK) to the culture medium 12 h after transfecting cells with the Meq plasmid. Subsequently, we analyzed cell lysates by sodium dodecyl sulfate-polyacrylamide gel electrophoresis and Western blotting. Pretreating the cells with a caspase-6-specific inhibitor blocked TYK2 degradation after transient Meq expression (Fig. 5-E), suggesting that TYK2 degradation during MDV infection was caspase-6-dependent, which in turn was dependent upon Meq.

We also examined the effects of caspase inhibitors on ISG production in infected cells. CEFs were pretreated with Z-VEID-FMK, infected with MDV for 24 h, and then treated with IFN-β for another 12 h. The caspase-6 inhibitor increased IFITM3 expression in IFN-treated cells during infection (Fig. 5-F), indicating that MDV suppressed IFN-β-dependent IFITM3 induction, which could be reversed by inhibiting caspase-6. These results suggest that Meq inhibited the JAK–STAT pathway by degrading TYK2 in a caspase-6-dependent manner.

3.6. Meq plays an important role in MDV immune evasion

Previous findings demonstrated that the Meq gene not only serves as the primary virulence factor of MDV but also plays crucial roles in viral replication and transmission. We conducted *in vivo* and *in vitro* experiments to assess the potential involvement of Meq in MDV immune evasion. As depicted in Fig. 6-A, MDV-dMeq showed significantly lower replication in CEFs than MDV-WT. It is widely acknowledged that MDV infection is initiated during the early cytolysis stage of 3–7 dpi, followed by an incubation period of 7–10 dpi. Given that innate immunity occurs primarily during the initial stages of viral infection, we monitored early changes in viral replication. In an *in vivo* experiment, 1-day-old chickens were infected with either the MDV-WT or MDV-dMeq strain, and viral replication and the expression levels of antiviral genes were examined at 7 dpi. As illustrated in Fig. 6-B, the loss of Meq weakened MDV replication to some extent during the early cytolysis stage. Moreover, chickens infected with MDV-dMeq exhibited significantly higher levels of *PKR*, *ZAP*, *Mx1*, and *IFITM3* than those infected with MDV-WT (Fig. 6-C). These findings strongly indicate that Meq serves essential roles in both viral replication and the immune-evasion mechanisms employed by MDV.

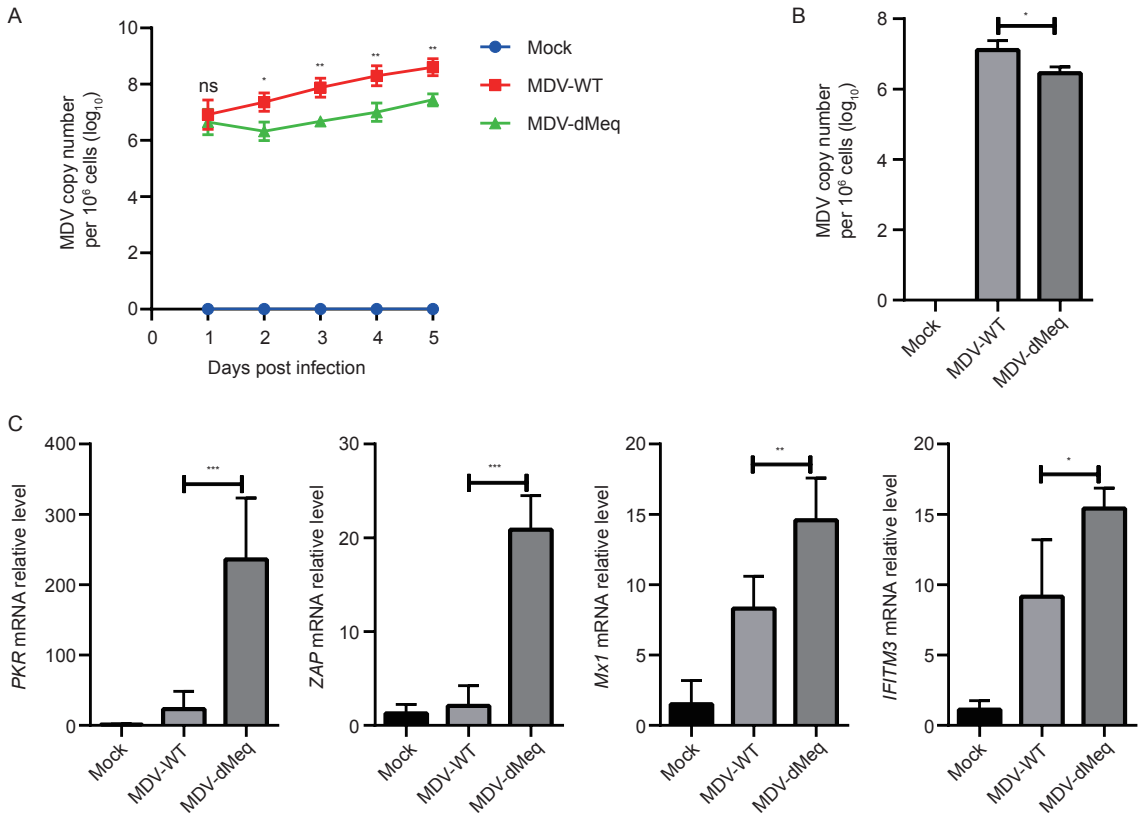


Fig.6 Effects of Meq deficiency on Marek's disease virus (MDV) replication and interferon-stimulated gene (ISG) production. A, embryonic fibroblasts (CEFs) were inoculated with MDV-Georgia srtain (GA) or MDV-dMeq, or mock-infected. The viral copy numbers were quantified by qPCR at the indicated time points after infection. B and C, 1-day-old chickens were infected with 2,000 PFUs of wild-type MDV (MDV-GA) or defective MDV (MDV-dMeq). Spleen samples were collected at 7 days post-infection to determine viral copy numbers (B) and the transcription levels of ISGs (C). *PKR*, protein kinase R; *ZAP*, zinc finger antiviral protein; *Mx1*, myxovirus resistance protein 1; *IFITM3*, interferon-induced transmembrane protein 3. Statistical significance is denoted as follows: *, $P<0.05$; **, $P<0.01$; ***, $P<0.001$; ns, no significant difference.

4. Discussion

MDV, a highly contagious and carcinogenic herpesvirus, induces immunosuppression in infected chickens, rendering them more susceptible to concurrent or secondary bacterial or viral infections (Heidari *et al.* 2016). However, the precise mechanisms underlying MDV-induced tumorigenesis and immunosuppression remain unclear. The current findings revealed that during the initial cytolytic phase of MDV infection in chickens, the MDV Meq protein inhibited the ISRE promoter activity of chicken ISGs, which effectively dampened the transcription and translation of ISGs, underscoring the ability of MDV to modulate the host immune response and enabling evasion of host surveillance and immunity. This modulation is crucial for viral reactivation and translation during infection. Further studies are warranted to ascertain whether MDV encodes proteins that suppress ISGs and to elucidate the underlying mechanisms.

The successful establishment and perpetuation of viral infections hinges on the ability of viruses to evade and modulate the intrinsic host immune response (Beachboard and Horner 2016). Viruses typically thwart IFN responses by impeding IFN induction, obstructing IFN-stimulated ISG induction, or both. Previous data have revealed that MDV thwarted IFN-β induction by counteracting the cGAS-STING pathway (Li *et al.* 2019). Conversely, the JAK–STAT signaling pathway is indispensable for IFN signaling to induce ISG effector proteins (Lin *et al.* 2004). Avian herpesvirus proteins that regulate the JAK–STAT pathway have been less studied than those of mammals. In this study, we constructed a library comprising over 100 MDV ORFs, which were screened for their capacity to substantially impede ISRE promoter activity in a high-throughput manner using a dual-luciferase reporter system. We found that MDV can elude the host innate immune response by influencing STAT1 phosphorylation and nuclear translocation, which is required for heterodimerization with phosphorylated STAT2 in order to bind the ISRE promoters of ISGs and regulate their expression (Best *et al.* 2005). Our findings provide primary evidence of an interaction between the major MDV oncoprotein, Meq, and JAK1 and TYK2.

The JAK–STAT pathway encompasses JAK1 and TYK2, which transmit IFN signals downstream and recruit STAT1 and STAT2 for phosphorylation. DNA and RNA viruses have acquired strategies for eliminating host defense mechanisms. For instance, human cytomegalovirus infection leads to a marked reduction in JAK1 protein levels, impeding ISG activation by diminishing the molecular foundation of the JAK–STAT pathway (Miller *et al.* 1998, 1999). Conversely, herpes simplex virus type 1 obstructs the phosphorylation of JAKs and STATs stimulated by IFN, while deactivating pathway components (Yokota *et al.* 2001). Our previous study identified the MDV oncoprotein Meq as an inhibitor of the cGAS-STING DNA-sensing pathway *via* interaction with STING and IRF7, which impaired IRF7 activation and IFN-β induction (Li *et al.* 2019). In the present study, the Meq protein was further shown to be capable of impeding the JAK–STAT signaling pathway, thereby inhibiting STAT1 phosphorylation and ISG production.

Proteins are typically degraded through ubiquitin-proteasome-dependent degradation, the autophagy-lysosome pathway, or caspase-mediated protein hydrolysis (Sun *et al.* 2021). Our results revealed that inhibiting the caspase-mediated protein hydrolysis pathway, but not the ubiquitin-proteasome or autophagy-lysosome signaling pathways, restored TYK2 levels in Meq-expressing cells. These findings implied that TYK2 degradation may occur through either an apoptotic or caspase-dependent pathway. A panel of caspases, including caspase-3, -4, -6, and -8, was selected for further analysis. Caspase-3 and -6 act as executioner caspases, whereas caspase-8 functions as an initiator caspase (Fan *et al.* 2005). By employing selective caspase inhibitors, we found that only a caspase-6-specific inhibitor impeded TYK2 degradation. This finding suggests that Meq-dependent TYK2 protein downregulation depends on caspase-6. When caspase-6 levels decreased, TYK2 degradation was reversed in MDV-infected cells. These findings indicate that Meq plays a direct role in circumventing the innate antiviral response after MDV infection.

5. Conclusion

In summary, our findings indicate that the MDV oncoprotein, Meq, plays a novel role in repressing ISG expression by selectively targeting JAK1 and TYK2 in the type-I IFN pathway. Meq directly bound to JAK1 and TYK2, which impeded the JAK1–STAT1 interaction and inhibited TYK2 degradation through a caspase-6-mediated apoptosis pathway. Thus, Meq impeded ISRE regulation and expression. The JAK–STAT pathway orchestrates the activation of a wide range of antiviral proteins and the eradication of pathogens *via* innate immunity. Meq may help induce tumorigenesis by obstructing the JAK–STAT signaling pathway and facilitating persistent infection. These results highlight the pivotal mechanism whereby MDV evades the host's innate immunity. These data deepen the understanding of the tumorigenic and immune-evasion mechanisms of MDV and lay the groundwork for developing more efficacious MDV vaccines.

Acknowledgements

This research was supported by grants from the National Natural Science Foundation of China (32270154, U20A2061), the Central Public-interest Scientific Institution Basal Research Fund, China (Y2022QC26), and the China Agricultural Research System (CARS-41-G15).

Declaration of competing interest

The authors declare that they have no conflict of interest.

Declaration of generative AI and AI-assisted technologies in the writing process

The authors declare that they did not use AI in the preparation and writing of this manuscript.

Ethical approval

This study was conducted in strict accordance with the recommendations of the Guide for the Care and Use of

Laboratory Animals from the Ministry of Science and Technology of China (MSTC 2017). The use of SPF eggs, embryos, and chickens, as well as the animal experiments, was approved by the Animal Ethics Committee of the Harbin Veterinary Research Institute of the Chinese Academy of Agricultural Sciences and was performed in accordance with animal ethics guidelines and an approved protocol (SYXK (Hei) 2017-009).

References

Beachboard D C, Horner S M. 2016. Innate immune evasion strategies of DNA and RNA viruses. *Current Opinion in Microbiology*, **32**, 113–119.

Best S M, Morris K L, Shannon J G, Robertson S J, Mitzel D N, Park G S, Boer E, Wolfinbarger J B, Bloom M E. 2005. Inhibition of interferon-stimulated JAK–STAT signaling by a tick-borne Flavivirus and identification of NS5 as an interferon antagonist. *Journal of Virology*, **79**, 12828–12839.

Brubaker S W, Bonham K S, Zanoni I, Kagan J C. 2015. Innate immune pattern recognition: A cell biological perspective. *Annual Review of Immunology*, **33**, 257–290.

Conradie A M, Bertzbach L D, Bhandari N, Parcells M, Kaufer B B. 2019. A common live-attenuated avian herpesvirus vaccine expresses a very potent oncogene. *mSphere*, **4**, e00658-19.

Darnell Jr J E, Kerr I M, Stark G R. 1994. Jak–STAT pathways and transcriptional activation in response to IFNs and other extracellular signaling proteins. *Science*, **264**, 1415–1421.

Davidson I. 2020. Out of sight, but not out of mind: Aspects of the avian oncogenic herpesvirus, Marek's disease virus. *Animals* (Basel), **10**, 1319.

Fan T J, Han L H, Cong R S, Liang J. 2005. Caspase family proteases and apoptosis. *Acta Biochimica et Biophysica Sinica*, **37**, 719–727.

Heidari M, Wang D, Delekta P, Sun S. 2016. Marek's disease virus immunosuppression alters host cellular responses and immune gene expression in the skin of infected chickens. *Veterinary Immunology and Immunopathology*, **180**, 21–28.

Jarosinski K W, Tischer B K, Trapp S, Osterrieder N. 2006. Marek's disease virus, lytic replication, oncogenesis and control. *Expert Review of Vaccines*, **5**, 761–772.

Johnson C L, Gale Jr M. 2006. CARD games between virus and host get a new player. *Trends in Immunology*, **27**, 1–4.

Katze M G, He Y, Gale Jr M. 2002. Viruses and interferon, a fight for supremacy. *Nature Reviews Immunology*, **2**, 675–687.

Levy A M, Gilad O, Xia L, Izumiya Y, Choi J, Tsalenko A, Yakhini Z, Witter R, Lee L, Cardona C J, Kung H J. 2005. Marek's disease virus Meq transforms chicken cells *via* the v-Jun transcriptional cascade, a converging transforming pathway for avian oncoviruses. *Proceedings of the National Academy of Sciences of the United States of America*, **102**, 14831–14836.

Li K, Liu Y, Xu Z, Zhang Y, Luo D, Gao Y, Qian Y, Bao C, Liu C, Zhang Y, Qi X, Cui H, Wang Y, Gao L, Wang X. 2019. Avian oncogenic herpesvirus antagonizes the cGAS-STING DNA-sensing pathway to mediate immune evasion. *PLoS Pathogens*, **15**, e1007999.

Lin R J, Liao C L, Lin E, Lin Y L. 2004. Blocking of the alpha interferon-induced Jak-Stat signaling pathway by Japanese encephalitis virus infection. *Journal of Virology*, **78**, 9285–9294.

Liu J L, Kung H J. 2000. Marek's disease herpesvirus transforming protein Meq, a c-Jun analogue with an alternative life style. *Virus Genes*, **21**, 51–64.

Liu J L, Lin S F, Xia L, Brunovskis P, Li D, Davidson I, Lee L F, Kung H J. 1999. Meq and V-IL8, cellular genes in disguise? *Acta Virologica*, **43**, 94–101.

Miller D M, Rahill B M, Boss J M, Lairmore M D, Durbin J E, Waldman J W, Sedmak D D. 1998. Human cytomegalovirus inhibits major histocompatibility complex class II expression by disruption of the Jak/Stat pathway. *Journal of Experimental Medicine*, **187**, 675–683.

Miller D M, Zhang Y, Rahill B M, Waldman W J, Sedmak D D. 1999. Human cytomegalovirus inhibits IFN-alpha-stimulated antiviral and immunoregulatory responses by blocking multiple levels of IFN-alpha signal transduction. *Journal of Immunology*, **162**, 6107–6113.

Morrow C, Fehler F. 2004. Marek's disease: A worldwide problem. In: Davison F, Nair V, eds., *Marek's Disease*, *an Evolving Problem*. Elsevier, Amsterdam, The Netherlands.

MSTC (Ministry of Science and Technology of China). 2017. *Guide for the Care and Use of Laboratory Animals of the Ministry of Science and Technology of China*. 3rd ed. Central People's Government of the People's Republic of China, Beijing.

Platanias L C. 2005. Mechanisms of type-I- and type-II-interferon-mediated signalling. *Nature Reviews Immunology*, **5**, 375–386.

Qian Z, Brunovskis P, Lee L, Vogt P K, Kung H J. 1996. Novel DNA binding specificities of a putative herpesvirus bZIP oncoprotein. *Journal of Virology*, **70**, 7161–7170.

Qian Z, Brunovskis P, Rauscher F, Lee L, Kung H J. 1995. Transactivation activity of Meq, a Marek's disease herpesvirus bZIP protein persistently expressed in latently infected transformed T cells. *Journal of Virology*, **69**, 4037–4044.

Reid S P, Leung L W, Hartman A L, Martinez O, Shaw M L, Carbonnelle C, Volchkov V E, Nichol S T, Basler C F. 2006. Ebola virus VP24 binds karyopherin alpha1 and blocks STAT1 nuclear accumulation. *Journal of Virology*, **80**, 5156–5167.

Ross N L. 1999. T-cell transformation by Marek's disease virus. *Trends in Microbiology*, **7**, 22–29.

Sun G R, Zhang Y P, Zhou L Y, Lv H C, Zhang F, Li K, Gao Y L, Qi X L, Cui H Y, Wang Y Q, Gao L, Pan Q, Wang X M, Liu C J. 2017. Co-infection with marek's disease virus and reticuloendotheliosis virus increases illness severity and reduces marek's disease vaccine efficacy. *Viruses*, **9**, 158.

Sun M, Lin Q, Wang C, Xing J, Yan K, Liu Z, Jin Y, Cardona C J, Xing Z. 2021. Enterovirus A71 2B inhibits interferon-activated JAK/STAT signaling by inducing caspase-3-dependent karyopherin-α1 degradation. *Frontiers in Microbiology*, **12**, 762869.

Wang C, Sun M, Yuan X, Ji L, Jin Y, Cardona C J, Xing Z. 2017. Enterovirus 71 suppresses interferon responses by blocking Janus kinase (JAK)/signal transducer and activator of transcription (STAT) signaling through inducing karyopherin-α1 degradation. *Journal of Biological Chemistry*, **292**, 10262–10274.

Weber F, Kochs G, Haller O. 2004. Inverse interference: How viruses fight the interferon system. *Viral Immunology*, **17**, 498–515.

Wu J, Chen Z J. 2014. Innate immune sensing and signaling of cytosolic nucleic acids. *Annual Review of Immunology*, **32**, 461–488.

Yokota S, Yokosawa N, Kubota T, Suzutani T, Yoshida I, Miura S, Jimbow K, Fujii N. 2001. Herpes simplex virus type 1 suppresses the interferon signaling pathway by inhibiting phosphorylation of STATs and Janus kinases during an early infection stage. *Virology*, **286**, 119–124.

Executive Editor-in-Chief Dongming Zhao
Managing Editor Yanyan Sun